JOURNAL OF MATERIALS SCIENCE 11 (1976) 723–730

The effect of microstructure on the toughness of ferritic nodular cast iron

S. NISHI, T. KOBAYASHI, S. TAGA
Department of Metallurgical Engineering, Nagoya University, Nagoya, Japan

The ductile–brittle transition behaviour in ferritic nodular cast iron appears to depend not only on chemical compositions but also on many microstructural variables. The ferrite grain diameter and the mean free path between graphite nodules are studied here as the main microstructural variables, and the effects of these on toughness are investigated mainly by the instrumented Charpy impact test. The results show that the transition temperature is lowered when the ferrite grain size or the mean free path is decreased. On the other hand, increase in the ferrite grain size or the mean free path leads to a rise in the upper shelf energy in the ductile fracture range. Equations to predict the dynamic lower yield load (P_y) and the maximum load transition temperature (T_{rPm}) are derived from the relation for steel dispersed with spheriodal carbides.

1. Introduction

Nodular irons exhibit a high strength of 600 to $1000\,N\,mm^{-2}$ in the as-cast condition and high ductility to 10 to 20% elongation in an annealed ferritic iron, although, in the latter case, a small reduction in strength is observed. Ferritic iron, with a low silicon content and containing about 1% Ni has been recommended for low temperature applications [1].

Mechanical properties, especially the ductile–brittle transition behaviour of the ferritic nodular iron are considered to be affected mainly by chemical compositions [2] and microstructural variables. If the chemical compositions of the ferritic nodular iron are the same, the degree of spheroidization, the size of the graphite nodule, inter-particle (nodule) spacing, and ferrite grain size are considered to be the important microstructural variables, and they seem to be closely related to the ductile–brittle transition behaviour in this type of iron.

However, only a limited amount of work on these problems has been undertaken [3, 4], and no systematic result has been obtained. Therefore, in the present study, the effects of several important microstructural variables such as the ferrite grain size and the mean planar inter-particle spacing (mpis) or the mean free path (λ)* on the toughness of the ferritic nodular iron have been investigated.

2. Experimental methods

2.1. Material

The melt with the composition shown in Table I was cast into Y-shaped moulds as shown in Fig. 1.

TABLE I Chemical composition of material (wt%)

C	Si	Mn	P	S	Cr	Mg
3.71	2.53	0.29	0.014	0.015	0.028	0.045

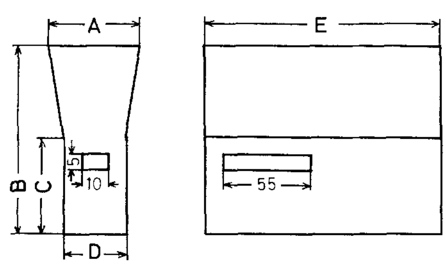

Mould No.	A	B	C	D	E
1	22.5	60	30	15	120
2	22.5	60	30	15	120
3	40	90	45	25	120
4	60	120	60	40	120

(mm)

Figure 1 Dimensions of Y blocks.

* The following relations are known. $\lambda = (1-f)/N$, and $\text{mpis} = (1/N_A)^{1/2} - (\pi/2)r$, where f is the volume fraction of particles, N is the number of particles which intersect a randomly oriented straight line of unit length, N_A is the number of particles per unit are, r is the average radius of particles. Data obtained in this study were analysed using λ.

TABLE II Data on dispersion of graphite nodules (λ) and ferrite grain size (*d*)

	Specimen							
	A1	B1	A2	B2	A3	B3	A4	B4
λ*	108†		119		140		166	
(cm × 10^{-4})	99.5	116.3	114.8	123.5	135.0	145.4	173.0	159.0
*D**								
(cm × 10^{-4})	35.6	19.8	43.4	21.9	54.0	26.8	47.2	26.0

* Microstructural parameters are the average of two or more determinations by the linear analysis technique.

† Rounded average value between specimens A1 and B1.

The mean free path in specimen A appeared a little larger than in specimen B.

To vary the nodule size and the mean free path, four different moulds were used, the dimensions of which are given in Table I and Fig. 1. Moulds 1 and 2 were identical in size but differ in that only the former had chill plates (size: 30 x 10 x 120 mm^3) on each side of the Y-shaped block.

To vary the ferrite grain size, the blocks cast into moulds were annealed to the ferritic condition by two methods of heat-treatment, A and B, i.e. heating at 950° C for 10 h or at 850° C for 5 h, respectively, followed by furnace cooling to 690° C and holding at this temperature for 24 h until finally cooling to room temperature. Charpy and tensile specimens were then machined out of the Y-shaped blocks.

The microstructure of all the specimens was completely ferritic after the heat-treatments mentioned above. The specimen code numbers, e.g. A1 or F4, used in this paper means, for example, heat-treatment A, or as-cast condition F, the numbers signifying the mould number.

2.2. Tensile tests and instrumented Charpy impact tests

Tensile tests were carried out at room temperature with specimen JIS No. 4. An unnotched specimen of the size 5 x 10 x 55 mm^3 was used as a Charpy specimen and the load–deflection relationship during impact was recorded by the instrumented Charpy test [5]. The test temperature range was +90 to − 196° C.

3. Experimental results

3.1. Microstructural characteristics

Quantitative data on microstructural characteristics of various specimens are given in Table II.

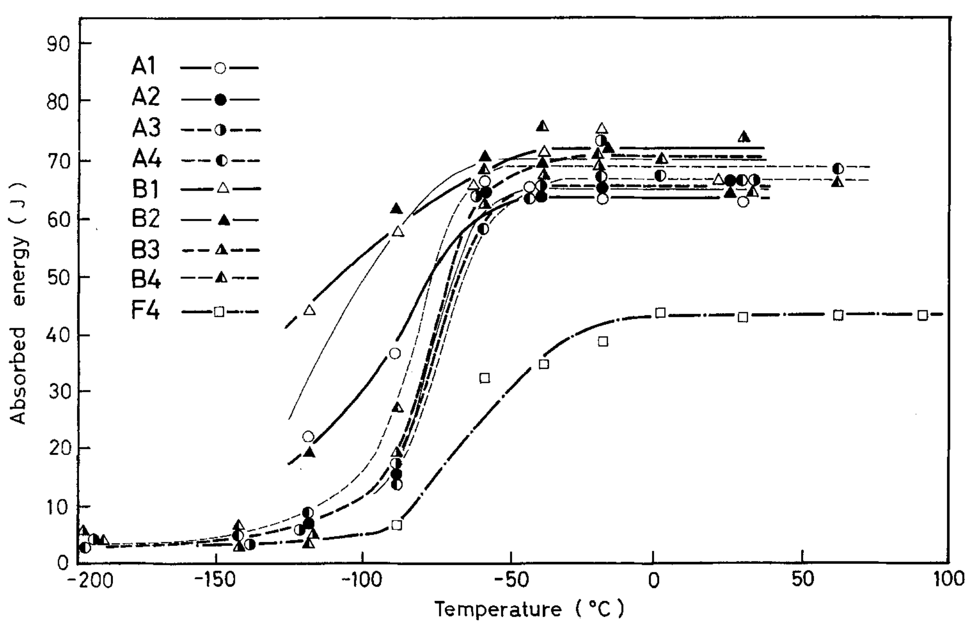

Figure 2 Result of Charpy impact test.

These values are the arithmetic means. The large and bimodal distribution in the sizes of λ and *d* were observed in every specimen, and it is, therefore, difficult to conduct a statistical analysis. It is inevitable, therefore, that some doubts should be placed on the value of the mean. It will be necessary to carry out some investigations on such problems in the future. It is evident from these data that the mean free path, λ, increases with decrease in the cooling rate during casting and solidification.

It is also noted that heat-treatment A, which

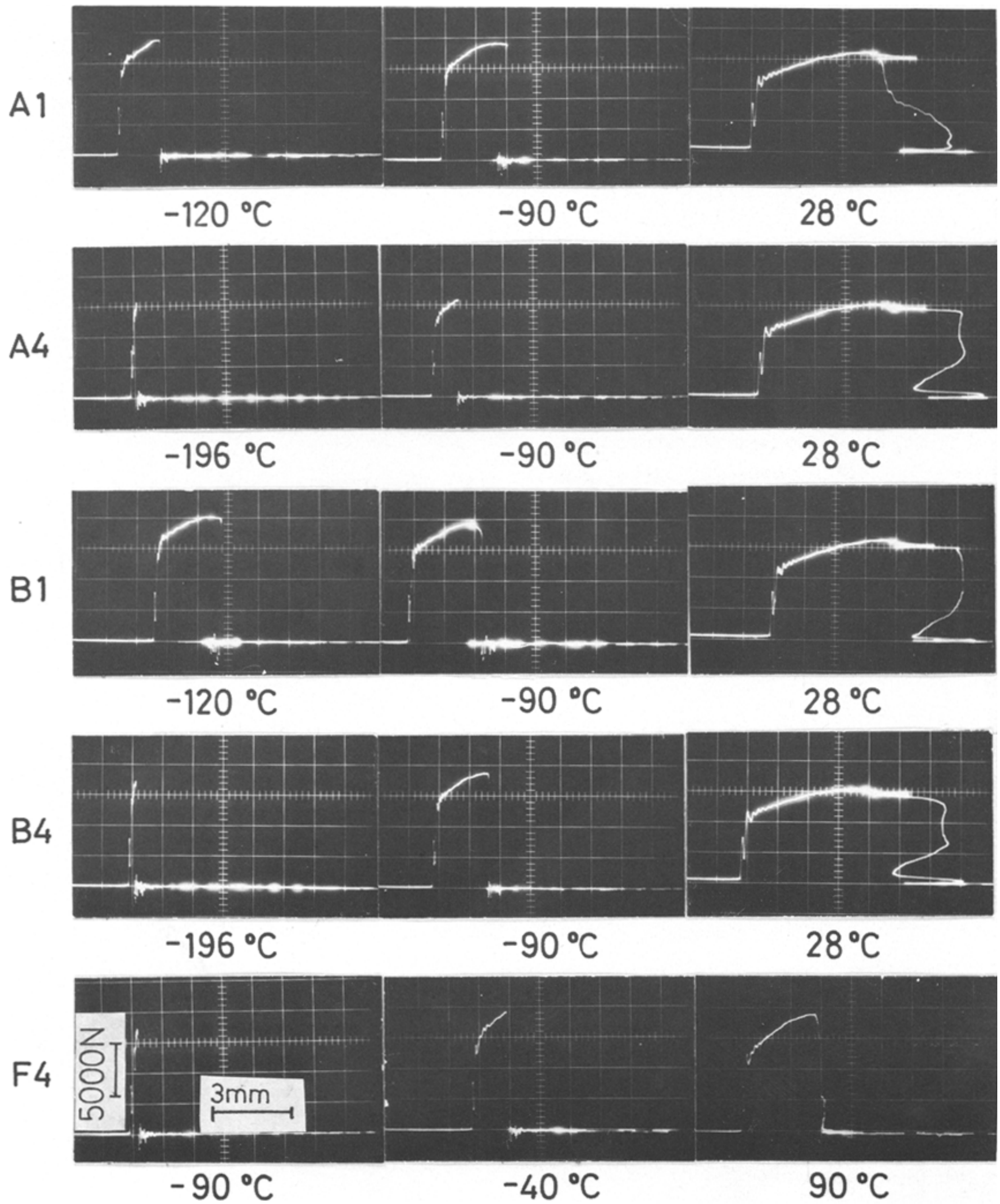

Figure 3 Typical load–deflection curves obtained from various specimens.

austenitizes for a longer time at higher temperatures, causes coarser grain size and a slightly larger mean free path than in heat-treatment B.

3.2. Results of tensile and instrumented Charpy impact tests

The result of the Charpy impact test is shown in Fig. 2. It is seen that the upper shelf energy of the as-cast specimen F4 in the ductile fracture range is rather low and that the transition temperature T_{rE} (transition temperature at which the energy level is lowered to half the upper shelf energy) is high. Most of the as-cast specimens used in this study exhibited a ferritic–pearlitic aggregate structure. Therefore, the above result may be explained by the view that the toughness in the nodular iron depends on the fraction of the ferrite in the matrix [6]. It is also observed that the specimens with fine ferrite grains (B1 and B2) show superior transition characteristics.

Some examples of the load–deflection curves recorded in the instrumented Charpy impact test are shown in Fig. 3. A typical load–deflection curve and various characteristic values used in the following analysis are shown in Fig. 4 [5, 7]. In the annealed iron, the specimen undergoes work-hardening between the lower yield load (P_y) and the maximum load (P_m), at which stage a fibrous crack is formed at the outer surface. The ductile crack then propagates slowly until unstable fracture occurs. Although inflections in the descending portion of the curve are observed, they are possibly due to the vibration of the hammer and the curve should be assumed to drop rapdily from the fracture load. The transition in absorbed energy with decreasing temperature usually occurs in two steps. The transition observed in the higher temperature range is the transition in E_p, i.e. the temperature at which E_p decreases to almost zero (T_{rP_m}, the temperature at which brittle fracture first appears at the maximum load P_m). In the lower temperature range, the transition in E_i is then observed.

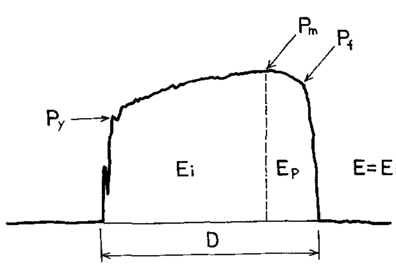

D : Deflection
P_y : Lower yield load
P_m : Maximum fracture load
P_f : Fracture load
E : Total absorbed energy
E_i : Crack initiation energy
E_p : Crack propagation energy

Figure 4 Typical illustration of load–deflection curves and various characteristic values used in the analysis.

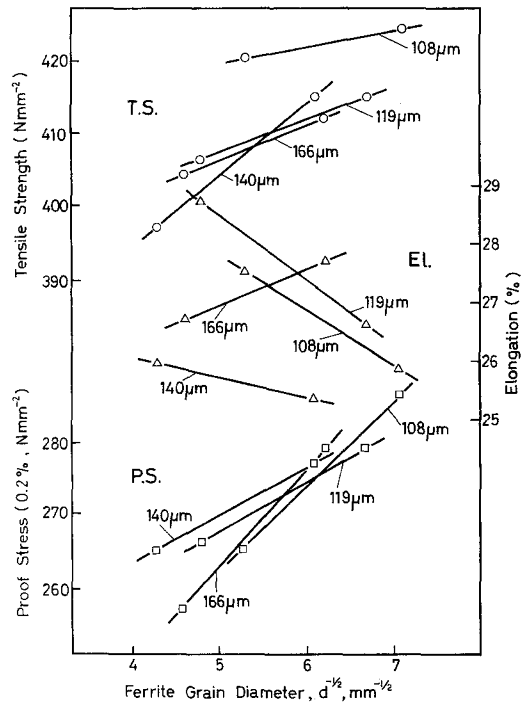

Figure 5 Effects of $d^{-1/2}$ and λ on tensile tests results.

There is no slow crack growth, however, in the case of as-cast specimen F; as a result of this, rapid transition to the brittle fracture appears immediately after crack initiation. For this reason the as-cast iron shows a low resistance to crack propagation.

Fig. 5 shows the relationship between tensile properties and microstructures. Both tensile strength and 0.2% proof stress increase with decrease in ferrite grain size, and this behaviour is well explained by Petch's equation [8]. It is seen in Fig. 5 that elongation decreases with grain refining with the exception of the largest value of λ (λ = 166 μm; the respective average value of λ for all specimens of the same number is given in the figure for convenience), where the elongation,

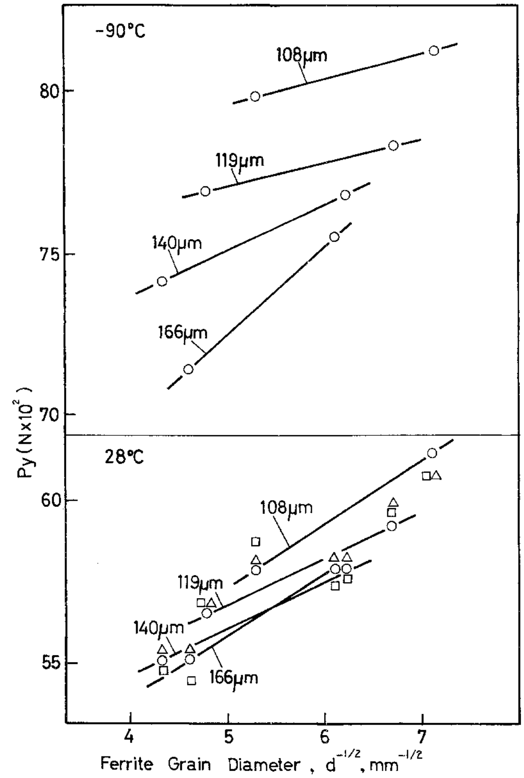

Figure 6 Effects of $d^{-1/2}$ and λ on P_y.

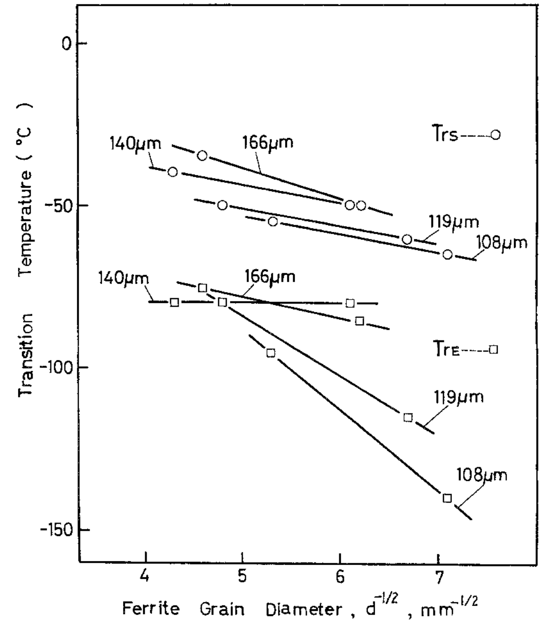

Figure 7 Effects of $d^{-1/2}$ and λ on T_{rs} and T_{rE}.

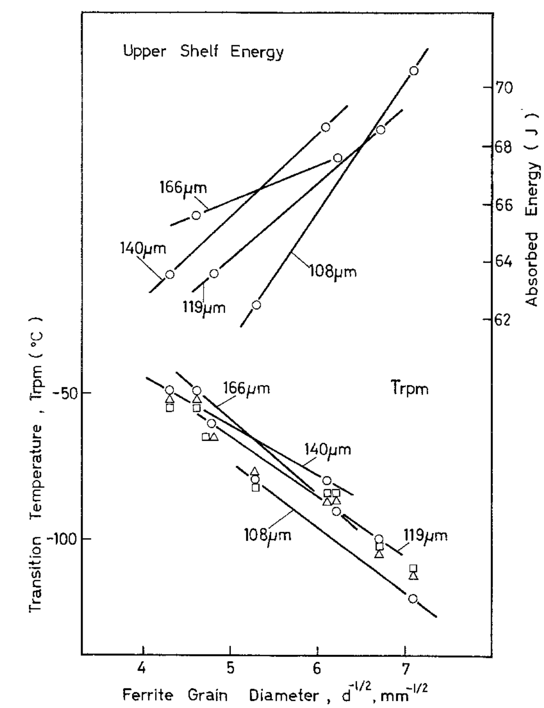

Figure 8 Effects of $d^{-1/2}$ and λ on T_{rP_m} and upper shelf energy.

as well as the strength, increases with increase in grain size. The tensile strength, on the other hand, shows a tendency to increase when λ is small.

Fig. 6 shows the relationship between P_y recorded in the instrumented Charpy impact test, and the microstructural variables. It is also observed that P_y increases with decrease in the grain size in a similar way to the proof stress shown in Fig. 5. This grain-size dependence is nearly the same at each test temperature; however, the absolute value of P_y is larger at low temperatures, as is expected from the temperature dependence of the yield strength. Higher P_y values are also observed when λ is small. The effects of the grain size and λ on P_y will be mentioned later.

The relationships between the transition temperatures and the microstructural variables are shown in Fig. 7. Both T_{rs} (50% ductile fracture facet transition temperature) and T_{rE} show a tendency to be lowered by refining the grain size and by decrease in λ. This tendency appears more clearly at the energy transition temperature T_{rE}.

Fig. 8 shows the relationships between T_{rP_m} and the upper shelf energy in the ductile fracture range with the microstructural variables. It is observed that T_{rP_m} is lowered by refining the grain size and by decrease in λ, in the same manner as T_{rs} and T_{rE} as shown in Fig. 7. The upper shelf energy in the ductile fracture range is observed to increase when the grain size is refined and λ is widened. The latter phenomenon has also been reported by Mogford *et al.* [3]. However, the increasing rate of the upper shelf energy against the $d^{-1/2}$ may be larger in the case of small λ values (see Fig. 8) and it seems that more studies on this aspect are necessary in the future.

4. Discussion

4.1. The effect of ferrite grain size on the toughness of ferritic nodular iron

Although the specimens used in this study were of only two grain sizes with similar λ values, the effect of grain size on toughness can be obtained by taking the result of various λ values into consideration.

The lower yield stress, σ_y, will be given by the well-known relation, $\sigma_y = \sigma_i + K_y \cdot d^{-1/2}$, derived by Petch [8]. Where, σ_i is the frictional stress for slip of free dislocations in a crystal, and K_y is a measure of the pinning of dislocations. It is understood from the equation that the yield stress rises with decreasing grain size. The result of the tensile test in this study has also shown the validity of the equation; that is, specimen B which has finer grain size than specimen A shows higher proof stress and tensile strength.

According to the results of the instrumented Charpy impact test, lowering of the transition temperatures, the rise in upper shelf energy, and improvement in the mechanical properties under the dynamic loading conditions have been observed. These results are interpreted on the basis of the Petch equation stated above, because the equation has been found to be applicable even in the impact test [9]. The relationship between the grain diameter (d) and the ductile–brittle transition temperature (T_c) is usually given by the following formula [10],

$$\epsilon \cdot T_c = \sigma_0^* + C - (4q\mu\gamma'/k^* - k^*)d^{-1/2},$$

where, ϵ, C, k^* are constants, σ_0^* is the frictional stress for slip, μ is rigidity modulus, γ' is surface energy for crack growth, q is a measure of triaxiality ($= \frac{1}{3}$ to 1).

In this equation, the transition temperature varies according to the values of d, σ_0^*, γ', q, and μ; but as long as a specified material is concerned, it is well-known from many studies that d has the largest influence on the transition temperature. It seems, therefore, that the results obtained in this study are well explained by the above discussions.

4.2. The effect of the distribution of graphite nodules on the toughness of ferritic nodular iron

According to the reported results, it is generally said that the graphite nodule can act as a site of ductile crack nucleation by its decohesion along the graphite–matrix interface or by the stress concentration induced by the piling up of dislocations near the interface (it may not be the interface itself [11]). Moreover the graphite nodule, in some cases, can act as an arrester against cleavage crack propagation [3, 7].

The test results show that the transition temperature is lowered with decrease in λ. This behaviour will be explained by the increase in the number of graphite nodules which will resist cleavage crack propagation (see Figs. 7 and 8). Moreover, if the graphite itself or the graphite–matrix interface is weak, a crack with a length of $2r$ will be nucleated in such a site and will propagate into the matrix when the following Griffith equation is satisfied:

$$\sigma_f = (E\gamma/2r)^{1/2},$$

where σ_f is the critical cleavage fracture stress, E is Young's modulus, r the radius of a graphite nodule, and γ the surface energy for cleavage fracture. This equation shows that the cleavage fracture stress depends on the nodule size and that the small nodule size will give superior brittle fracture strength.

On the other hand, the energy absorption in the ductile fracture range shows higher values when the graphite nodule size or the value of λ is larger. The same result has also been reported by Gilbert [12]. Gurland and Plateau [13] have studied the effect of spherical inclusions on the mechanical properties of metallic materials. According to their report, the true fracture strain, ϵ_f, can be given as follows: $\epsilon_f = \epsilon_0 + \frac{1}{3} \ln [1 + \frac{3}{2}(k_2^2/k_1)(\lambda^2/r)]$; where, ϵ_0 is true fracture strain when particles, or their interfaces, fracture, r is the radius of a particle, λ, in this case, is the mean planar interparticle spacing (mpis) defined in this study, k_1, k_2 are constants. In the case of a spherical particle, mpis can be given by $\frac{4}{3}r\,[(1-f)/f]$, therefore, ϵ_f depends only on the volume fraction of the particles, f.

In the present study, however, the volume fraction of the nodules is constant (f is 0.12) and then ϵ_0 does not seem to greatly vary with r. Therefore, the ductile fracture characteristic in the present results cannot be explained by the above equation. Another interpretation described below seems to be preferable for understanding the role of the graphite nodules in the ductile fracture characteristic of the ferritic nodular iron. According to the fractographic observations, the fracture surface consists of macroscopic dimple patterns which were formed by the decohesion-like fracture along the nodule–matrix interface [7]. Therefore, it may be assumed that the increase in the number of graphite nodules or the refining of the nodule size results in the increase in ductile crack nucleating sites. This results in the reduction of the matrix area at fracture. The decrease in the ductile fracture energy induced by the refining of the nodule size seems to occur according to such a fracture process.

In the studies on spheroidal steel, Orowan [14] reported that the yield stress increased proportionally with λ^{-1} and, on the other hand, Ansell *et al.* [15] reported that it was proportional to $\lambda^{-\frac{1}{2}}$ when the dispersion was relatively coarse. From examination of such studies conducted by Conrad *et al.* [17] has shown that the yield stress, σ_y, can be given in the simplified form of $\sigma_y = A + B\lambda^{-1} + Cd^{-1/2}$ (where A, B and C are constants). It is interesting to know whether such a relation is or is not observed even in the case of nodular iron, because in this case, the particle (nodule) size is equal to or larger than the ferrite grain size and the coherency between the graphite and the matrix is poor; moreover, the strength of the graphite itself is low.

The result on the effects of λ and d on P_y is shown in Fig. 5. Both the models of Orowan and Ansell *et al.* were investigated. The dependence of P_y on λ^{-1} was obtained at room temperature as follows: P_y (N) $= 4237 + 70.1\,\lambda^{-1}$ (mm^{-1}) $+ 172\, d^{-1/2}$ (mm$^{-1/2}$) (symbol □ in the figure). From the view of the dependence on $\lambda^{-1/2}$, on the other hand, the following relation can be derived: P_y (N) $= 4295 + 179.5\lambda^{-1/2}$(mm$^{-1/2}$)$+ 172 d^{-1/2}$(mm$^{-1/2}$) (symbol △ in the figure). In these equations, the first term reflects the dependence of the yield strength on temperature, strain-rate and chemical composition. The second and the third terms depend on the distribution of the graphite nodules and the ferrite grain size, respectively.

The mean values evaluated from the above two equations and the one determined from the experiments (symbol ○ in the figure) show good agreement. It is assumed, therefore, that the ductility in the nodular cast iron is mainly influenced by the mean free path, λ, and the grain size, d. However, it is difficult to say whether the effect $\lambda^{-1/2}$ and λ^{-1} is superior (a similar result has also been reported in for steel [17]. Further research will be necessary in order to clarify this.

The same factor was also considered for transition temperature T_{rP_m} (see Fig. 8). As a result, the following equations have been derived: T_{rP_m} (° C) $= 74 - 15.8\,\lambda^{-1/2}$ (mm$^{-1/2}$) $- 19.5\, d^{-1/2}$ (mm$^{-1/2}$) (symbol △ in the figure) or T_{rP_m} (° C) $= 57 - 3.4\,\lambda^{-1}$ (mm^{-1}) $-$ $19.5\, d^{-1/2}$ (mm$^{-1/2}$) (symbol □ in the figure). These values are also seen to agree well with the experimental values. From these results, it is clear that P_y or T_{rP_m} in the ferritic nodular iron can be determined quantitatively from the microstructural variables, λ and d.

5. Conclusions

(1) The transition temperature is lowered as the ferrite grain size or the spacing between the graphite nodules is decreased.

(2) The ductile fracture energy in the upper shelf range is raised when the ferrite grain size is small or the spacing between the graphite nodules is large. The latter case is explained as follows: when the size of the graphite nodule is large, the number of the void nucleating sites for ductile crack initiation decreases and, moreover, the net sectional area of the specimen increases.

(3) The role of the graphite nodule in the brittle fracture is considered to be two-fold; the first is the role in the brittle crack initiation stage and the second the role in the propagation stage. In the initiation stage, it is considered that the increase in the number of graphite nodules (the decrease in the spacing between graphite nodules) causes a decrease in the unit crack length initiated at the graphite nodule and it finally leads to a lowering of the transition temperature. In the propagation stage, the graphite nodules resist brittle crack propagation. Therefore, the increase in the number of nodules may lower the transition temperature.

(4) The yield stress (σ_y) or transition temperature (T_c) in ferritic nodular iron can be expressed by the well-known relation for spheroidal carbon steel, i.e.

$$\sigma_y = A + B\lambda^{-1} + Cd^{-1/2}, \quad T_c = A - B\lambda^{-1} - Cd^{-1/2}$$

where A, B and C are constants, λ is the spacing between graphite nodules and d the ferrite grain diameter. This relation was established in this study and the values obtained agreed well with those determined from the experiment. $\lambda^{-1/2}$ may also be applied instead of λ^{-1}.

(5) It is concluded from these results that the most desirable microstructure from the viewpoint of toughness is the fine ferrite grain structure with a relatively fine dispersion of the graphite nodules.

Acknowledgement

The authors wish to express their sincere thanks to Professor A. Otsuka of Nagoya University for his valuable discussions and critical reading of the manuscript.

References

1. G. J. COX, *Foundry Trade J.* **131** (1971) 833.
2. S. NISHI, T. KOBAYASHI and S. TAGA, *Imono* **48** (3) (1976).
3. I. L. MOGFORD, I. L. BROWN and D. HULL, *JISI* **205** (1967) 729.
4. G. N. J. GILBERT, *Brit. Foundrymen* **14** (1961) 5.
5. T. KOBAYASHI, K. TAKAI and H. MANIWA, *Trans. ISIJ* 7 (1967) 115.
6. W. S. PELLINI *et al.*, *Trans ASM* **46** (1954) 418.
7. T. KOBAYASHI, *Tetsu-to-Hagane* **59** (1973) 1578, *Trans. ISIJ* **16** (3) (1976).
8. N. J. PETCH, *JISI* **174** (1953) 25.
9. S. SAKUI and T. MORI, *Nippon Kinzoku-gakkai-ho* **3** (1964) 358.
10. N. J. PETCH, "Fracture" (Wiley, New York, 1959) p.54.
11. A. OTSUKA, *Res. Rep. Fac. Eng. Hiroshima Univ.* **10** (1961) 241.
12. G. N. J. GILBERT, *BCIRAJ* **15** (1964) 590.
13. J. GURLAND and J. PLATEAU, *Trans. ASM* **56** (1963) 442.
14. E. OROWAN, "Dislocations in Metals" (AIME, New York, 1954) p.69.
15. G. S. ANSELL and F. V. LENEL, *Acta Met.* **8** (1960) 612.
16. H. CONRAD, "Iron and its dilute solid solutions" (Interscience, New York, 1963) p.314.
17. T. KUNITAKE, *Tetsu-to-Hagane* **54** (1968) 710.

Received 31 July and accepted 3 October 1975.